Latency of Fluid Antenna Systems

Adrian Evans

***Abstract*—Mobile communication devices like smartphones, tablets and smartwatches benefit from having multiple internal antennas as far apart as possible to reduce the spatial correlation between receiving antennas and increase channel capacity. However, the small form factor of such devices means that a substantial separation distance is not practical. Fluid antenna systems are an emerging technology in which the physical position of a reconfigurable antenna can be changed to pick up the best signal. We consider a fluid antenna system for a mobile device in which a slug of liquid metal can move to different positions or 'ports' in an electrolyte-filled tube. In response to the spatial variation in signal strength along the length of the tube, algorithms are designed to control the channel selection and movement of the slug. We benchmark the performance of a single-tube system against a fixed-location antenna. Simulation results and analysis demonstrate that the conventional fixed-location antenna outperforms the single-tube system due to the latency in transmission caused by the slug's movement. As a result, two modifications were explored to reduce latency. First, the fixed antenna is made available as a backup to address the outage during slug movement. Secondly, a novel two-tube fluid antenna system was designed to separate the transmission and channel selection functions into different tubes.**

***Index Terms*—Fluid antenna system, latency, channel estimation, port selection algorithms.**

I. Introduction

A. Project motivation

MODELLING wireless communication channels is challenging because wireless channels change over time and vary with location. Signals sent from a base station arrive at an antenna of a mobile communication device along multiple paths, especially in urban or indoor environments. This multipath propagation is due to objects, such as buildings or walls, that reflect and scatter the signal. These reflections can destructively interfere with each other and introduce phase shifts, time delays, attenuations and distortions that reduce the signal-to-noise ratio (SNR). Because of this dynamic environment, two antennas at different locations or the same antenna at different times can receive completely different signals. However, having multiple antennas can significantly improve the mobile device's reliability. The risk that every antenna in a device receives a terrible signal is reduced through antenna diversity. This results in an improved SNR, which can be used to increase the channel's capacity. Additionally, if there are multiple antennas on both the mobile device and the base station, a multiple input multiple output (MIMO) system is formed that can increase channel capacity even further.

Given that the SNR and channel capacity increase with the number of antennas, manufacturers of mobile devices want to use as many internal antennas as possible. However, there is a limit. If antennas are located too close to each other, the channel correlation increases because the antennas will receive increasingly similar signal components, and consequently, the capacity decreases. It has been deduced that the antennas on a mobile device will be significantly more correlated if spaced apart by less than half of the received signal's wavelength, i.e., $d_{\min} \approx \lambda/2$ [1]. Accordingly, smartphone antennas are typically fixed into positions in the device's four corners to provide as much separation as possible. However, the small form factor of such devices means that adding an antenna between two preexisting antennas is impossible. Additionally, it is not always practical to reduce the size of the antennas to increase the separation distance. Supporting evidence for a plateau in antennas per smartphone can be seen in Apple's iPhones, which have had no more than 4×4 MIMO (four antennas for sending and receiving data) since the iPhone XS and XS Max release in 2018. Apple would be incentivised to add antennas to its smartphones since it would result in better performance through increased channel capacity. For example, a study by *PC Magazine* showed that the iPhone 11 Pro with 4×4 MIMO had double the maximum download speed of the iPhone 11 with 2×2 MIMO, i.e., only two antennas for sending and receiving data [2].

A solution to the problem of limited space in mobile devices may lie in a reconfigurable antenna that provides antenna diversity through the ability to move the antenna to one of many positions in the device rather than a limited number of fixed positions at least half a wavelength apart. Fluid antenna systems (FAS) are a recently proposed technology by Wong *et al.* for 6G [3]. In a FAS, the physical position of a reconfigurable antenna can be changed to one of N positions or 'ports' along a fixed-length line space to pick up the best signal, such as, the strongest signal or least interference. As there is no minimum inter-port distance, the FAS can occupy a small space with a large number of ports. The exact number of ports will depend on the system's ability to deliver incremental movement of the antenna. The rationale behind FAS is to obtain the benefits of antenna diversity from many ports rather than from fitting many antennas within a small space. Accordingly, a FAS is a potential candidate for use in mobile devices instead of conventional fixed-location antennas. One proposed architecture involves mobilising a liquid-metal slug in an electrolyte-filled tube with a voltage pulse [4].

To be included in 6G, a FAS must have a simple yet effective algorithm to control the channel selection and movement of the liquid-metal slug within the tube. One approach is to observe the channel at every port and then choose the optimal port with the highest channel gain. This paper investigates the efficiency of such a method through simulations. We also propose modifications to reduce latency in transmission caused by the slug's movement.

This project was supervised by Pawel Dmochowski and Peter Smith. The author would like to thank them for their help, support and encouragement.

B. Project goals

The aim of this project was to investigate the latency of a fluid antenna system through simulations. There were four major goals:

1) develop a model for a fluid antenna system housed in a mobile communication device and used in an urban environment;
2) design an algorithm to control the movement of a liquid metal slug in a tube of the fluid antenna system, such that the slug will observe the channel at each port before moving to the optimal port with the highest channel gain for transmission;
3) analyse the algorithm's efficiency in terms of the SNR and benchmark the fluid antenna system's performance against:
   a) a perfect fluid antenna system in which the slug's speed is infinite; and
   b) a conventional fixed-location antenna operating in the same device;
4) use the findings to propose design improvements to future fluid antenna systems given that this area is still in its infancy.

C. Performance metrics

The SNR is the primary performance metric in wireless communication systems, as it measures the ratio of signal power to noise power, i.e.,

$$\text{SNR} = \frac{\text{signal power}}{\text{noise power}}. \tag{1}$$

For linear system models, like the one under study, there are two definitions of SNR that can be used: the average power SNR and the instantaneous power SNR [5]. The appropriate performance metric for evaluating the effect of antenna diversity is instantaneous power SNR rather than taking the average SNR over multiple antennas. Instantaneous power SNR is defined as

$$\text{SNR}_{\text{instant}} = \frac{P_{\text{instant}}}{\sigma^2}, \tag{2}$$

where P_{instant} is the instantaneous signal power and σ^2 is the average noise power. The specific channel capacity, C, can then be calculated as an SNR rate by

$$C = \log_2\left(1 + \text{SNR}_{\text{instant}}\right). \tag{3}$$

D. Sustainability

This project contributes towards the United Nations' Sustainable Development Goal (SDG) No. 7 of ensuring sustainable energy use by modelling a fluid antenna system that aims to improve the energy efficiency of the communications network by increasing its capacity [6]. Although 6G research has only recently begun, it has been speculated that its target will be cutting the average power consumption of networks in half compared to 5G while still supporting peak channel capacities ten times greater than today's 5G networks [7].

This project also contributes to SDG No. 12 of ensuring sustainable consumption and production, including minimising the adverse effects on human health and the environment from toxic chemicals and mining. Using non-toxic gallium-based metal alloys (such as Galinstan or Eutectic Gallium-Indium) instead of toxic mercury for the liquid metal slug is better for people's health and the environment. Gallium is not mined but is a byproduct of producing other metals, such as aluminium [8]. As a result, aluminium smelters, such as New Zealand's smelter at Tiwai Point near Bluff, collect gallium while converting bauxite into alumina and could be used to supply the metal without any additional environmental impact.

E. Tools and methodology

There were two options for analysing the algorithm's performance: numerically using simulations or analytically using communications engineering theory. Both options were explored, but numerical simulations using Matlab proved to be a more straightforward method. Papers that carry out analysis must make non-physical simplifications as a proper analysis appears impossible.

II. Literature review

The literature reviewed for this project gave the necessary information to make informed decisions about the design of the model and algorithm. This section discusses the current state of the art in fluid antenna systems and liquid metal antennas.

A. Fluid antenna systems

Fluid antenna systems were first proposed by Wong *et al.* in 2020 [3]. The authors demonstrated that, even in a small space, a single-antenna FAS can outperform a multiple-antenna maximum ratio combining (MRC) system in terms of outage probability if the number of ports is large enough. In the hypothesised FAS, the single antenna could switch positions instantly for the best performance. However, instantaneous slug movement is unrealistic, and the authors recognised that significant obstacles need to be overcome before FAS can play a role in 6G, including reducing the response time to switching and designing port selection algorithms [4]. This initial work was extended into multi-user communications, where a mathematical framework was introduced that considers multiple pairs of transmitters and FAS-based receivers [9]. However, the authors continued to assume that any delay in switching between the ports was negligible and could be ignored. Although unrealistic, a "perfect" slug with infinite speed is a useful benchmark for comparing the performance of a slug with a realistic speed, as it shows the best possible performance of the FAS.

The large number of ports in FAS and the complexity of observing every port have prompted the development of port selection algorithms that observe only a subset of ports and infer the best port. Chai *et al.* proposes several algorithms that utilise a combination of machine learning methods and analytical approximation to identify the optimal port in a single-user system [10]. Waqar *et al.* has done the same for a multiuser network [11]. Similarly, Wang *et al.* proposes an

algorithm based on the least squares regression to identify the optimal port [12].

Skouroumounis *et al.* have proposed a system comprising a circular array of M tubes arranged so as to extend longitudinally outwards from the centre, with a $\frac{2\pi}{M}$ angle between adjacent tubes [13]. Rather than estimate the channel at each port, the system uses a sequential linear minimum mean-squared error (LMMSE)-based channel estimation method on only a few ports by leveraging the strong spatial correlation between ports in adjacent tubes. This system appears to have some disadvantages. First, the system reduces the signalling overhead at the cost of reducing the SNR. Secondly, the circular array of tubes is bulky and difficult to house in the small form factor of a smartphone, tablet or smartwatch. In contrast, the channel estimation methods under study in this project aim to improve the SNR and, by utilising far fewer tubes, is considerably less bulky for the same number of ports per tube.

B. Liquid metal antennas

The idea behind FAS was motivated by the increasing trend of using liquid metals for antennas. The term liquid metal refers to metals that are liquid at room temperature, namely, mercury (Hg), cesium (Cs), rubidium (Rb) and gallium (Ga). Of these metals, gallium has received the most attention as an antenna because, unlike mercury, it is non-toxic and, unlike cesium and rubidium, it does not readily oxidise in air or react violently with water [8]. Gallium has a melting point of 29.8°C. However, the melting point of a gallium-based alloy (such as Galinstan or Eutectic Gallium-Indium) can be made lower than this through the addition of other post-transition metals, such as indium (In), tin (Sn) or lead (Pb).

Tubes or channels of various shapes and sizes are usually required to contain and control liquid metals. Microfluidic tubing is often utilised when miniaturisation is desired, while thermoplastic tubing is typically used for commercial applications due to its low manufacturing cost [14]. The techniques for moving a slug of liquid metal through a tube or channel can be classified as pneumatic, magnetic, thermal or electrical. The electrical techniques are further classified as electrocapillary, electrowetting on dielectric (EWOD), continuous electrowetting (CEW), and electrochemically controlled capillary (ECC) [15]. Each of these electrical techniques involves manipulating the interfacial tension of the liquid metal slug by applying an electrical potential between a pair of electrodes.

Electrical actuation techniques are often preferred to other techniques because they do not require bulky components like a micropump, magnet or heater. Instead, most electrical actuation techniques only need a pair of electrodes (one at each end of the tube) and an electrolyte within the tube. However, coating the surface of the liquid metal slug with charged nanoparticles can increase its actuating speed. Tang *et al.* carried out a study in which a Galinstan slug was coated in WO_3 nanoparticles and placed in a channel filled with electrolyte solutions [16]. At a voltage of 15 V across the electrodes, the slug moved to the end of the channel at a speed of 100 mm/s, which is 1.25 times faster than that of the uncoated slug under the same conditions.

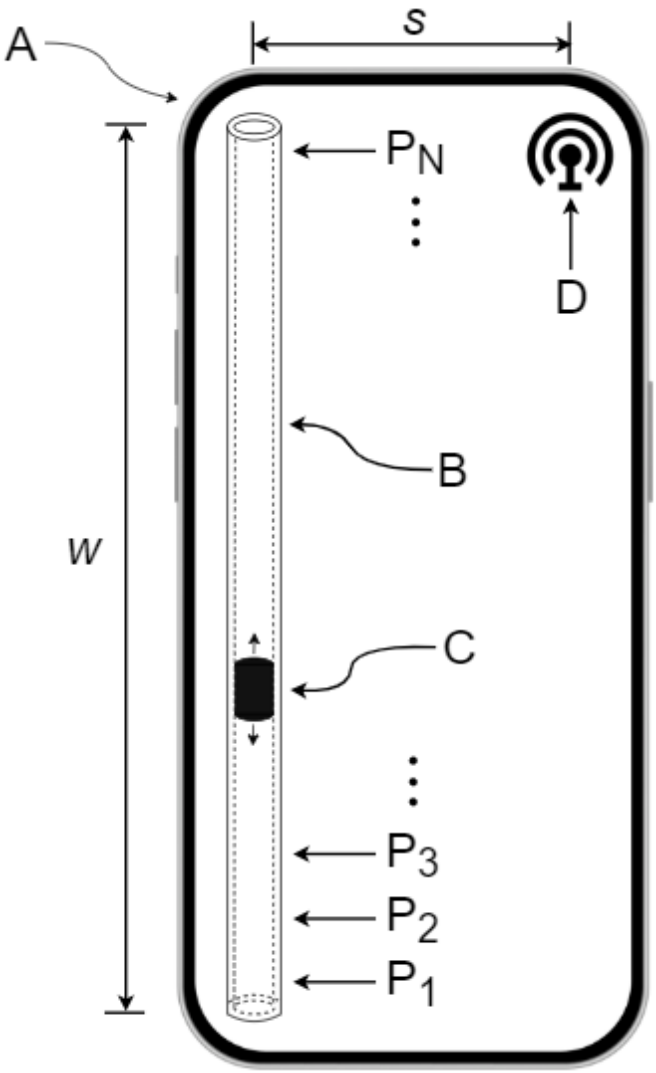

Fig. 1. Physical architecture of the modelled system.

III. Model design and implementation

In this section, we present the design of the modelled fluid antenna system and discuss its implementation. First, we outline the physical architecture of the system model in part A, followed by a description of the port selection algorithm in part B and the benchmarks used for comparing the algorithm's performance in part C.

Secondly, we delve into the components of the model itself, providing detailed discussions on implementing the following aspects: sample times (part D), multipath fading channels (part E), temporal correlation (part F), spatial correlation (part G), and spatio-temporal correlation (part H).

The code for the model has been made available on the GitLab repository [17] .

A. Physical model

Fig. 1 depicts the physical architecture of the modelled fluid antenna system. As shown in the Fig. 1, the system is housed inside a mobile communication device (marked as A), such as a smartphone. The FAS comprises an electrolyte-filled tube

(B) in which a liquid metal slug (C) can move to one of N evenly distributed ports (P_1, P_2, P_3, … P_N) along the length w of the tube. Consistent with United Nations' SDG No. 12 of ensuring sustainable consumption and production, the slug is made from a gallium alloy (such as Galinstan) rather than mercury, so it is non-toxic and available as a byproduct of producing other metals without any additional mining. The slug moves through the tube upon exposure to a voltage pulse across a pair of electrodes (not shown), one at each end of the tube. The polarity and amplitude of the voltage pulse control the slug's direction and speed of movement. The distance δ between the ports is given by

$$\delta = \frac{w}{N-1}. \quad \text{[m]} \quad (4)$$

The slug cannot move and transmit at the same time. Therefore, as a backup to the FAS, the mobile device contains a conventional fixed-location antenna (D), which can transmit continuously. The concept of a backup antenna is in keeping with the United Nations' SDG No. 9, relating to building resilient infrastructure. The fixed antenna is spaced a minimum distance s from the tube. As the separation distance s decreases, the spatial correlation between the ports in the tube and the fixed antenna increases. A high spatial correlation makes it more likely that the signal that the slug in the tube receives is similar to the signal that the fixed antenna receives. Indeed, if s is zero and the fixed antenna is overlayed on top of a port in the tube, the signals received by that port and the fixed antenna will be identical.

B. Port selection algorithm

An algorithm was developed to control the movement of the liquid metal slug, such that the slug will observe the channel at each of the N ports before moving to the optimal port with the highest channel gain for transmission.

The steps in the algorithm are:

1) initialise the slug at a randomly selected port in the tube;
2) unless already at one end, move the slug to the closest end of the tube;
3) observe the channel at the endmost port;
4) move the slug to the other end of the tube and, at each of the N-1 ports along the way, observe the channel;
5) move the slug to the optimal port with the highest channel gain;
6) stay at the optimal port while transmitting; and
7) repeat steps 2 to 6.

C. Benchmarks

The algorithm set out above will be carried out by a slug with a selected speed for moving between ports and a selected time for observing the channel at each port by waiting for pilot signals to be received from the base station. These delays will negatively impact the performance of the FAS but provide valuable information about the likely real-world implementation of the system. For comparison purposes, the performance of this "imperfect" system will be compared with a "perfect" system without these delays. In the perfect FAS, the slug always knows the optimal transmission port without observing any of the channels. Additionally, the slug of the perfect system can instantaneously move to the optimal port without delay. Therefore, unlike the imperfect system, the perfect system can transmit continuously. In contrast, the slug of the imperfect system can only transmit for a selected period before a new cycle of the algorithm is run.

As well as the perfect system, the other benchmark for comparison with the imperfect system is a conventional fixed-location antenna. As shown in Fig. 1, the fixed antenna (D) is mounted in the upper right-hand corner of the device (A). Like the perfect system, the fixed antenna can transmit continuously. However, unlike either FAS, the fixed antenna cannot take advantage of antenna diversity because it is a single antenna. Accordingly, the fixed antenna provides an interesting comparison with the imperfect system as they each possess an advantage over the other.

D. Sample times

Instead of using units of time to determine how long the steps in the algorithm take to complete, the simulation counts the number of samples taken. Each sample has a sample period T_s, the inverse of which is the sample rate R_d, i.e., $T_s = \frac{1}{R_\mathrm{d}}$. The maximum sample count for the slug to complete steps 2 to 6 (or one cycle) is given by

$$S_\mathrm{max} = \frac{5}{2} S_\mathrm{m}(N-1) + N S_\mathrm{o} + S_\mathrm{t}, \quad (5)$$

where S_m is the sample count for the slug to move from one port to an adjacent port, S_o denotes the sample count for the slug to observe the channel at each port, and S_t denotes the sample count for the slug to transmit at the optimal port. It can be seen from (5) that the most significant contributor to S_max is S_m, with 2.5 traversals of the tube required in the worst-case scenario. S_m is given by

$$S_\mathrm{m} = \frac{\delta}{v_\mathrm{s} T_\mathrm{s}}, \quad (6)$$

where v_s is the slug's speed (controlled by the voltage pulse across the electrodes at either end of the tube).

The channel observation sample count S_o is the second biggest contributor to S_max and is determined by the number of slots available to receive pilot signals from the base station. Finally, the transmission sample count S_t is determined by

$$S_\mathrm{t} = \frac{T_\mathrm{t}}{T_\mathrm{s}}, \quad (7)$$

where T_t is the transmission time and the solution of

$$J_0\left(2\pi F_\mathrm{d} T_\mathrm{t}\right) = C_\mathrm{t}, \quad (8)$$

where $J_0(\cdot)$ is a Bessel function of the first kind and zeroth order, F_d denotes the maximum Doppler shift, and C_t denotes a chosen coherence target. The maximum Doppler shift, F_d, is given by

$$F_d = \frac{v_\mathrm{u} f}{c}, \quad \text{[Hz]} \quad (9)$$

where f is the signal's carrier frequency, v_u is the speed of the user of the mobile device, and c is the speed of light. v_u

can vary significantly depending on whether the mobile device user is, for example, a pedestrian or a passenger in a moving vehicle.

The coherence target C_{t} is the chosen threshold level of temporal correlation (between 0 and 1) corresponding to the time, T_{c}, over which the channel can be assumed to be constant. The coherence time T_c is inversely proportional to the maximum Doppler spread of the channel, i.e.,

$$T_{\mathrm{c}} \propto \frac{1}{F_{\mathrm{d}}}. \tag{10}$$

As a result, signals that have less than the coherence time T_{c} of the channel are received approximately undistorted by the effects of Doppler spread and, therefore, mobile speed [18].

In a similar manner to (5), the minimum sample count for the slug to complete steps 2 to 6 of the algorithm (or one cycle), which involves a single traversal of the tube in the best-case scenario, is given by

$$S_{\min} = S_{\mathrm{m}}(N-1) + NS_{\mathrm{o}} + S_{\mathrm{t}}. \tag{11}$$

E. Multipath fading channels

Rayleigh and Rician fading channels are useful models of real-world phenomena in wireless communications, including multipath scattering effects, time dispersion, and Doppler shifts that arise from relative motion between the transmitter and receiver. While Rician fading occurs when there are direct and indirect paths between the transmitter and receiver, Rayleigh fading occurs when there is no direct path and only indirect paths between the transmitter and receiver. A Rayleigh fading channel is therefore a worst-case channel. Rayleigh fading was selected to model the multipath fading channels as the mobile device will be used in an urban environment where there is unlikely to be a direct path or line-of-sight between the mobile device and a base station. The decision to model the mobile device being used in an urban environment rather than a rural or open-space environment where it would perform better due to a direct line-of-sight to the base station finds support in United Nations' SDG No. 11, relating to making cities inclusive, safe, resilient and sustainable.

$N+1$ Rayleigh fading channels (one for each of the N ports in the FAS and one for the fixed-location antenna) were implemented using the Matlab built-in function `rayleighchan`. This function takes in R_{d} and F_{d}, both discussed above, and a sum-of-sinusoids model for temporal correlation and provides a received signal with Rayleigh fading amplitude and random phase shifts.

F. Temporal correlation

Mobile communication devices must be able to cope with changes in signal quality over time caused by the movement of either the device or scattering objects in the propagation environment. This time-variant behaviour will mean that the optimal port for transmission (i.e., the port with the highest channel gain) will change over time. Therefore, the $N+1$ Rayleigh fading channels must evolve such that each port's channel gain at one sampled instance in time is temporally correlated with that port's channel gain at the next.

Using a 'for' loop, multiple outputs of the `rayleighchan` function are captured in a $(N+1) \times numTimeSteps$ temporal correlation matrix $\mathbf{H}_{\mathrm{t}}$, where $numTimeSteps$ denotes the number of sampled time instances. Each of the $N+1$ rows in $\mathbf{H}_{\mathrm{t}}$ is temporally correlated using a sum-of-sinusoids model in which Doppler components in the time domain are added together to generate the time domain fading envelope.

G. Spatial correlation

A large spatial correlation between signals at antenna elements is undesirable since it decreases the effectiveness of antenna diversity. An essential step in modelling the ports is, therefore, to establish a relationship between port spacing and the correlation coefficient. Several spatial correlation matrix models have been proposed in the literature. For example, the exponential correlation model assumes that the correlation decreases exponentially with the distance between the antennas, i.e., the elements of the spatial correlation matrix $\mathbf{R}$ are $r_{ij} = a^{-d_{ij}}$, where d_{ij} is the distance between the antennas and $0 < a < 1$. However, this is an oversimplified model with no physical motivation [19].

In contrast to the exponential correlation model, the Jakes' model is both physically based and simple, making it ideal for a preliminary study [20]. The Jakes' model assumes a uniform distribution of multipath arrival angles such that the elements of the $(N+1) \times (N+1)$ spatial correlation matrix $\mathbf{R}$ are given by

$$r_{ij} = J_0\left(2\pi f_{\mathrm{s}} d_{ij}\right). \tag{12}$$

where f_{s} is a selected spatial correlation parameter.

As scattering objects surround a mobile communication device in an urban environment, a uniform probability density function (PDF) of $[0, 2\pi]$ will approximate the angular distribution of scatterers. Accordingly, the assumption underpinning the Jakes' model appears reasonable, and it was selected to model the spatial correlation. The Euclidean distance d_{ij} between the i^{th} and j^{th} ports is given by

$$d_{ij} = \sqrt{(x_j - x_i)^2 + (y_j - y_i)^2}. \tag{13}$$

The spatial parameter f_{s} in (12) is inversely proportional to the amount of correlation and is the solution of

$$J_0\left(2\pi f_{\mathrm{s}} \frac{\lambda}{2}\right) = \rho_{0.5}, \tag{14}$$

where $\rho_{0.5}$ denotes a chosen $\frac{\lambda}{2}$ correlation target, i.e., the correlation between two ports separated by half of the received signal's wavelength.

H. Spatio-temporal correlation

A combined spatio-temporal correlation matrix $\mathbf{H}_{\mathrm{st}}$ is produced using the simple and physically based Kronecker correlation model, since this model's underlying assumption that the correlation between the receive antennas is independent of the correlation among the transmit antennas appears reasonable [21], i.e.,

$$\mathbf{H}_{\mathrm{st}} = \mathbf{R}^{1/2}\mathbf{H}_{\mathrm{t}}. \tag{15}$$

The resulting $(N+1) \times numTimeSteps$ spatio-temporal correlation matrix $\mathbf{H}_{\text{st}}$ is effectively a lookup table that the port selection algorithm can utilise to determine the instantaneous signal power, P_{instant}, at any sampled time instance, i.e.,

$$P_{\text{instant}} = \rho^2(t), \qquad \text{[W]} \quad (16)$$

where $\rho^2(t)$ is the magnitude squared. With a selected and constant σ^2, the instantaneous power SNR can then be calculated using (2).

The following examples will show how $\mathbf{H}_{\text{st}}$ may be used as a lookup table to determine P_{instant}. In the first example, the slug of the imperfect tube is at step 4 of the algorithm and observes the channel at each tube port. If the slug observes the channel at port 15 and the sample count since the algorithm began running is 100, the magnitude at row 15, column 100 of $\mathbf{H}_{\text{st}}$, is looked up. If the slug only takes one sample count to observe the channel at each port (i.e., S_{o} = 1), then this magnitude squared is the observed P_{instant} at this port. If it takes more than one sample count to observe the channel at each port (i.e., $S_{\text{o}} > 1$), the magnitude at row 15, column 101 and so on, of $\mathbf{H}_{\text{st}}$ is also looked up, and an average magnitude squared becomes the port's P_{instant}. In this way, each port is allocated a P_{instant}, which can be sorted to determine the optimal port for transmission, i.e., the port with the greatest P_{instant}. In step 5 of the algorithm, the slug will travel to the optimal port for transmission (even if, due to the channel having changed in the meantime, it is no longer the optimal port by the time the slug arrives at this port). When the slug is transmitting during step 6 of the algorithm, the magnitude is again looked up in $\mathbf{H}_{\text{st}}$ for each transmission sample count, S_{t}, and from these magnitudes squared, the instantaneous power SNR values are calculated using (2).

Calculating the instantaneous power SNR values for the perfect tube is more straightforward than for the imperfect tube. Because the perfect tube's slug can change ports instantaneously and always to the optimal port with the highest channel gain, the P_{instant} at each sample count is the square of the highest magnitude in rows 1 to 50 for each column. With the same σ^2 used for the imperfect tube, the instantaneous power SNR values for the perfect tube are also calculated using (2). Finally, the instantaneous power SNR values for the fixed location antenna are the most straightforward to calculate. The P_{instant} at each sample count is the square of the magnitude in row 51 for each column. Again, using the same σ^2 as for the imperfect and perfect tubes, the instantaneous power SNR values are calculated using (2).

IV. Simulation results and evaluation

In this section, we present simulation results to evaluate the performance of the modelled FAS – also referred to as the "imperfect tube" – compared to two benchmarks discussed in Section III. These benchmarks are as follows:

1) an ideal FAS, or the "perfect tube", where the slug always possesses knowledge of the optimal transmission port and can instantaneously move to it; and
2) a conventional fixed-location antenna mounted in the upper right-hand corner of the mobile device, as illustrated in Fig. 1.

Unlike the FAS under study, both benchmarks transmit continuously, as opposed to periodically, over a specified transmission time T_{t}. Additionally, we will assess the performance of the FAS against two deployment scenarios related to the fixed-location antenna. Each deployment scenario is detailed below.

A. Imperfect tube or fixed antenna

In the first deployment scenario, the imperfect tube FAS is used alternately with the fixed-location antenna. Preference is given to the FAS due to its ability to take advantage of antenna diversity. Since the imperfect tube system can't transmit continuously, the fixed-location antenna is used as a backup antenna when the FAS is not transmitting, i.e., when the slug of the imperfect tube is carrying out any step in the algorithm other than step 6.

B. Imperfect tube and fixed antenna

In the second deployment scenario, we simultaneously utilise the imperfect tube FAS and the fixed-location antenna. At each time instance, we calculate these devices' combined instantaneous signal power by multiplying the P_{instant} from the FAS with that of the fixed antenna. This combined value is then fed into (2) to determine the instantaneous power SNR. The fixed antenna will always contribute a P_{instant} to the combined total, while the imperfect tube FAS will only do so periodically when transmitting.

C. Simulation parameters

As set out in Table I and discussed in Section III, the simulation parameters were selected to ensure a realistic model for evaluating the performance of the imperfect tube FAS. For example, the lengths w and s were chosen to conform to the dimensions of a large smartphone. Similarly, f was set to 3.5 GHz, aligning with the sub-6GHz range recommended as particularly suitable for FAS [3]. This frequency band was the primary band used in many of the world's first 5G networks that became operational in 2019 and may be repurposed for 6G in the future [22]. Although the slug's speed, v_{s}, of 1 ms^{-1} is ten times faster than a Galinstan slug coated in nanoparticles can currently travel [16], this speed is likely to increase with future research. The speed, v_{u}, of the mobile device user was set to a slow pedestrian walking speed of 1 kmh^{-1}.

D. Performance metrics

The capacity of a channel refers to the upper limit on the rate at which information can be transmitted over the channel. Accordingly, channel capacity is an invaluable performance metric. The normalised capacity of a channel is given by (3) and depends upon the instantaneous power SNR, a parameter that changes with time along with the channel. However, we can gain insights from multiple simulation cycles by utilising cumulative distribution function (CDF) capacity plots to aggregate capacity values. CDF capacity plots have become a vital tool in communications engineering, enabling comparisons between diverse time-variant systems and facilitating a deeper understanding of their performance under varying conditions.

TABLE I
TABLE OF SIMULATION PARAMETERS

Parameter	Value
Number of ports N	50
Tube length w	0.15 m
Port separation distance δ	0.02 m
Tube to fixed antenna minimum separation distance s	0.07 m
Sample period T_t	$5e^{-7}$ s
Sample rate R_d	$2e^{6}$ Hz
Slug movement sample count S_m	6,122
Slug observation sample count S_o	1
Slug transmission sample count S_t	44,205
Slug speed v_s	1 ms^{-1}
Maximum Doppler shift F_d	3.2 Hz
Coherence target C_t	0.95
Mobile device user speed v_u	1 kmh^{-1}
Signal's carrier frequency f	3.5 GHz
No. sampled time instances $numTimeSteps$	$1e^{6}$
Spatial correlation parameter f_s	194.3
Correlation target $\rho_{0.5}$	0.3
Average noise power σ^2	10 dB

E. Simulation results with a slug speed of 1 m/s

Fig. 2 plots the CDFs of specific channel capacity for the imperfect FAS tube. The instantaneous power SNR is computed using (2), and subsequently, the specific capacity is determined using (3). Additionally, we include CDFs for the two benchmarks: the perfect FAS tube and the fixed-location antenna. Furthermore, the two deployment scenarios involving the imperfect tube are represented: one where it is combined with the fixed antenna and the other where they are alternated.

The specific channel capacity of the imperfect tube is within the range of 0-1 bits per second (bps) and notably less than the perfect tube or the benchmarks and deployment scenarios. Unsurprisingly, the perfect tube demonstrates the best performance, boasting a channel capacity approximately six times greater than the imperfect tube's. Between these extremes is the benchmark involving the fixed antenna and the deployment scenarios. There is little to separate this group of three. However, as shown in the close-up in Fig. 2, the best performer of the trio is the combination of the imperfect tube with the fixed antenna. This is followed by the alternating use of the imperfect tube or fixed antenna and, finally, by the fixed antenna.

An examination of the minimum sample count, S_min, using (11) reveals that, at best, the imperfect tube is transmitting for 12.8% of the time ($S_\mathrm{t}/S_\mathrm{min} \times 100$) and not transmitting for the remaining 87.2% of the time. Similarly, an examination of the maximum sample count, S_max, using (5) reveals that, at worst, the imperfect tube is transmitting for 5.6% of the time ($S_\mathrm{t}/S_\mathrm{max} \times 100$) and not transmitting for the remaining 94.4% of the time. In contrast, the benchmarks and deployment scenarios transmit 100% of the time.

The low channel capacity of the imperfect channel can be attributed to its intermittent transmission characteristics. Specifically, the imperfect channel is active for a relatively small percentage of time, between 5.6% and 12.8% of the time. Most of the time, the slug of the imperfect channel is either in transit between ports or engaged in the observation of the channel at a specific port, rather than actively transmitting data. This infrequent transmission, coupled with the extended periods of non-transmission, contributes to the limited channel capacity observed in this simulation. The imperfect tube's intermittent transmission behaviour limits its ability to realise the benefits to channel capacity associated with antenna diversity. In contrast, the continuous transmission of the perfect tube enables it to fully exploit the gains in channel capacity that antenna diversity provides.

The impact of the imperfect tube's intermittent transmission is also evident in the performance of the two deployment scenarios compared to the fixed antenna alone. While both combinations involving the fixed antenna and the imperfect tube did result in a slightly higher channel capacity than the fixed antenna operating in isolation, the improvement in both cases was relatively modest. This limited enhancement is primarily attributed to the imperfect tube's intermittent transmission behaviour, which restricts its contribution to the channel capacity in both scenarios. This is also evident in the slight increase in channel capacity observed when the imperfect tube is used in conjunction with the fixed antenna instead of being used alternately.

F. Simulation results with varying slug speeds

Fig. 3 examines how the slug's speed impacts the imperfect tube's channel capacity. Four different slug speeds were investigated: 10 ms^{-1} in subplot (a), 20 ms^{-1} in subplot (b), 30 ms^{-1} in subplot (c), and 100 ms^{-1} in subplot (d). Aside from altering the slug speed, v_s, and the corresponding sample count, S_m, for the slug to move between adjacent ports, all other simulation parameters, as outlined in Table 1, remained consistent. The relationship between S_m and v_s is given in (6). The same two benchmarks of the perfect tube and the fixed antenna were used to compare the performance of the imperfect tube.

As slug speed increases, the channel capacity of the imperfect tube improves and approaches the upper limit given by the perfect tube, allowing more data to be received by the mobile device. The following observations were made:

At a slug speed of 10 ms^{-1}, the imperfect tube transmitted between 37% and 60% of the time (S_m = 612), and its channel capacity was approximately one-third of the perfect tube. It can be seen from the small amount of overlap between the capacity CDFs of the imperfect tube and the fixed antenna that the imperfect tube's performance at this slug speed falls short of regularly surpassing the fixed antenna.

At a slug speed of 20 ms^{-1}, the imperfect tube's transmission time increased to between 54% and 74% (S_m = 306). This led to a channel capacity roughly half that of the perfect tube. At this speed, the imperfect tube's channel capacity often surpassed the fixed antenna's.

With a slug speed of 30 ms^{-1}, the imperfect tube transmitted between 64% and 81% of the time (S_m = 204), resulting in a channel capacity of approximately two-thirds of the perfect tube. However, the channel capacity of the imperfect tube was now almost always superior to that of the fixed antenna.

At the highest slug speed of 100 ms^{-1}, the imperfect tube transmitted between 85% and 93% of the time (S_m = 61).

While its channel capacity was about 20% less than the perfect tube, as shown by the lack of any overlap between the capacity CDFs, the channel capacity of the imperfect tube always outperformed that of the fixed antenna.

G. Conclusion from simulations

The simulation results underscore the pivotal role of slug speed in determining the channel capacity of a FAS. Our findings suggest that, for FAS to regularly surpass the performance of a conventional fixed-location antenna, a minimum slug speed of at least 20 ms^{-1} is required.

V. Future work

As highlighted in the preceding section, our findings suggest that for a FAS to consistently outperform a conventional fixed-location antenna, a minimum slug speed of at least 20 ms^{-1} is imperative. However, this threshold speed significantly exceeds the current state of the art, where liquid metal slug speeds are about 0.1 ms^{-1} [16]. While it is reasonable to anticipate future advancements in slug speed, it is equally prudent to explore modifications to reduce the latency in transmission caused by the slug's movement, as it is the primary source of delay in the system. One such modification is to make the fixed antenna available as a backup to address the outage during slug movement, either in addition to or alternately with the FAS. Our results show that this can substantially improve the overall system's channel capacity, even with a slug speed as low as 1 ms^{-1}. Another promising modification involves the implementation of a novel two-tube FAS, which will be discussed below.

A. Novel two-tube FAS

Fig. 4 depicts the physical architecture of a modified version of the modelled fluid antenna system shown in Fig. 1. Like the modelled system, the modified version is housed inside a mobile communication device (marked as A), such as a smartphone. However, the modified FAS comprises two electrolyte-filled tubes (B1 and B2), spaced apart by a distance s, in which a pair of liquid metal slugs (C1 and C2) can move to one of N evenly distributed ports (P_1, P_2, P_3, … P_N) along the length w of each tube. As before, each slug moves through its tube upon exposure to a voltage pulse across a pair of electrodes (not shown), one at each end of the tube. The polarity and amplitude of the voltage pulse control each slug's direction and speed of movement, such that each slug can move independently of the other.

Compared to the modelled single-tube system, one of the chief advantages of the dual-tube system is its ability to enable one slug to search for the optimal transmission port while the other slug is actively transmitting. This concurrent operation should improve the system's channel capacity by minimising latency. When the tube separation distance, s, is small, the ports in both tubes should be highly spatially correlated. This high degree of spatial correlation is advantageous when one slug's role is dedicated to searching while the other slug's role is dedicated to transmission. However, maintaining highly spatially correlated tubes becomes undesirable if either slug can assume the searching and transmitting functions. Increasing s in such cases is advisable to decrease the spatial correlation between the tubes.

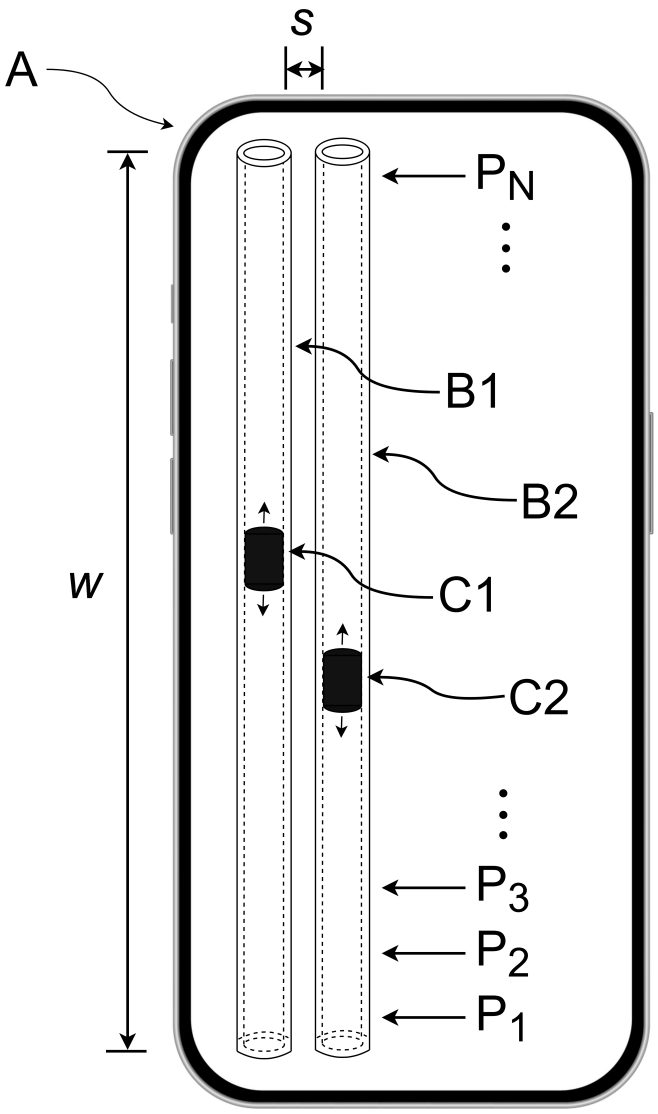

Fig. 4. Physical architecture of the modified system.

B. Modified algorithm

A further improvement to address the issue of latency would be to amend the port selection algorithm so that, rather than have the slug search for the optimal port with the highest channel gain, the slug instead searches for a port with a channel gain that is significantly higher than that currently used by the FAS for transmission, e.g., a gain at least 10% higher. Such an algorithm would reduce the movement of the slug and should, therefore, improve the FAS's performance.

VI. Conclusion

In this study, we modelled a fluid antenna system within a mobile device to investigate latency. Our study benchmarked

the performance of this system against a perfect fluid antenna system with no delay in transmission and a conventional fixed-location antenna. The results and subsequent analysis revealed a notable gap in channel capacity between the modelled system and the benchmarks, primarily due to the inherent latency in transmission caused by the slug's movement.

In response to the latency challenge, we explored two key modifications. The first involved the introduction of a fixed antenna as a backup to address outages during slug movement. This modification improved channel capacity significantly. Furthermore, we presented a novel solution of a two-tube fluid antenna system that separates the functions of transmission and channel selection into distinct tubes, optimising the system's overall efficiency.

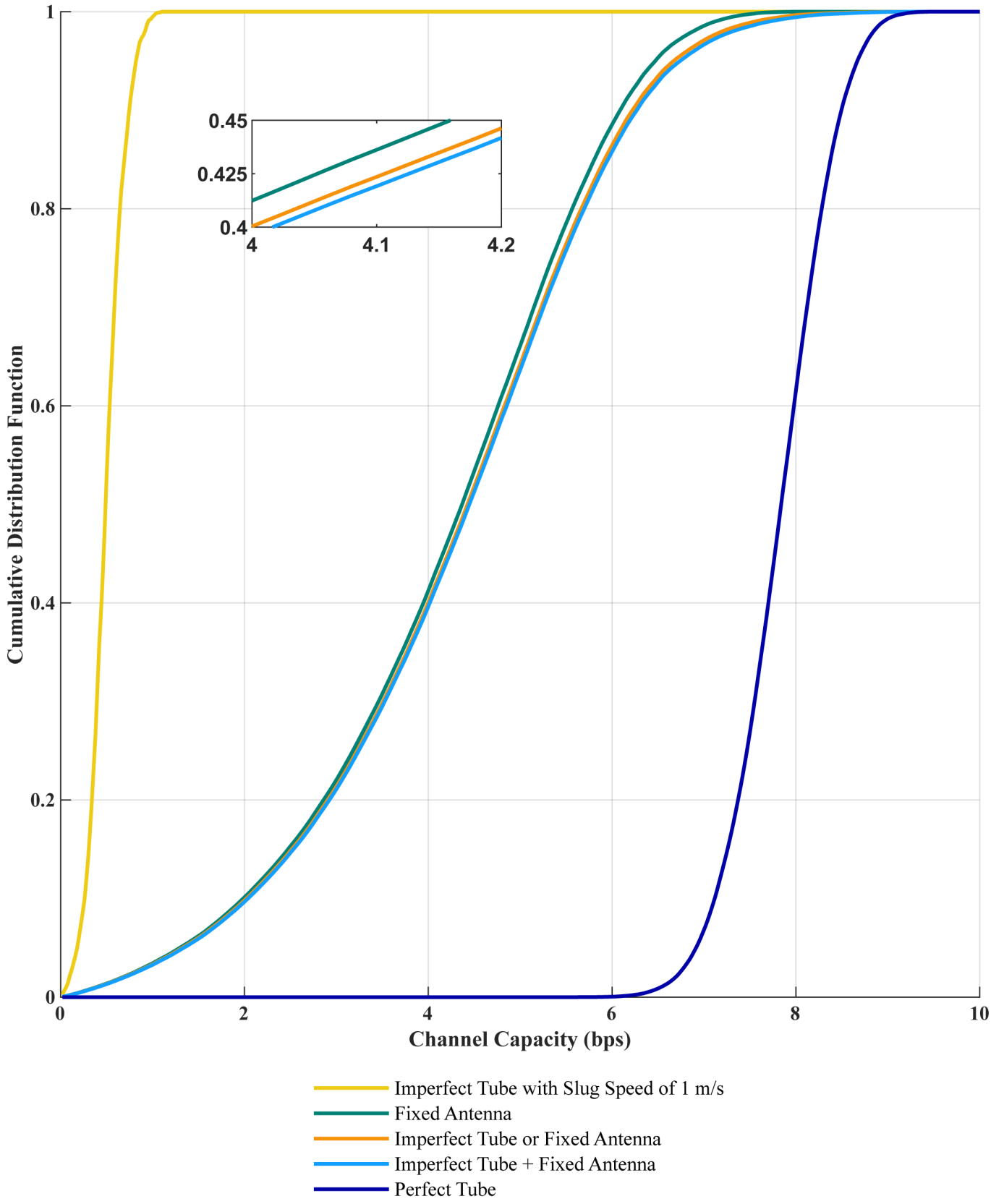

Fig. 2. Simulation results with the slug speed of the imperfect tube set to 1 ms^{-1}.

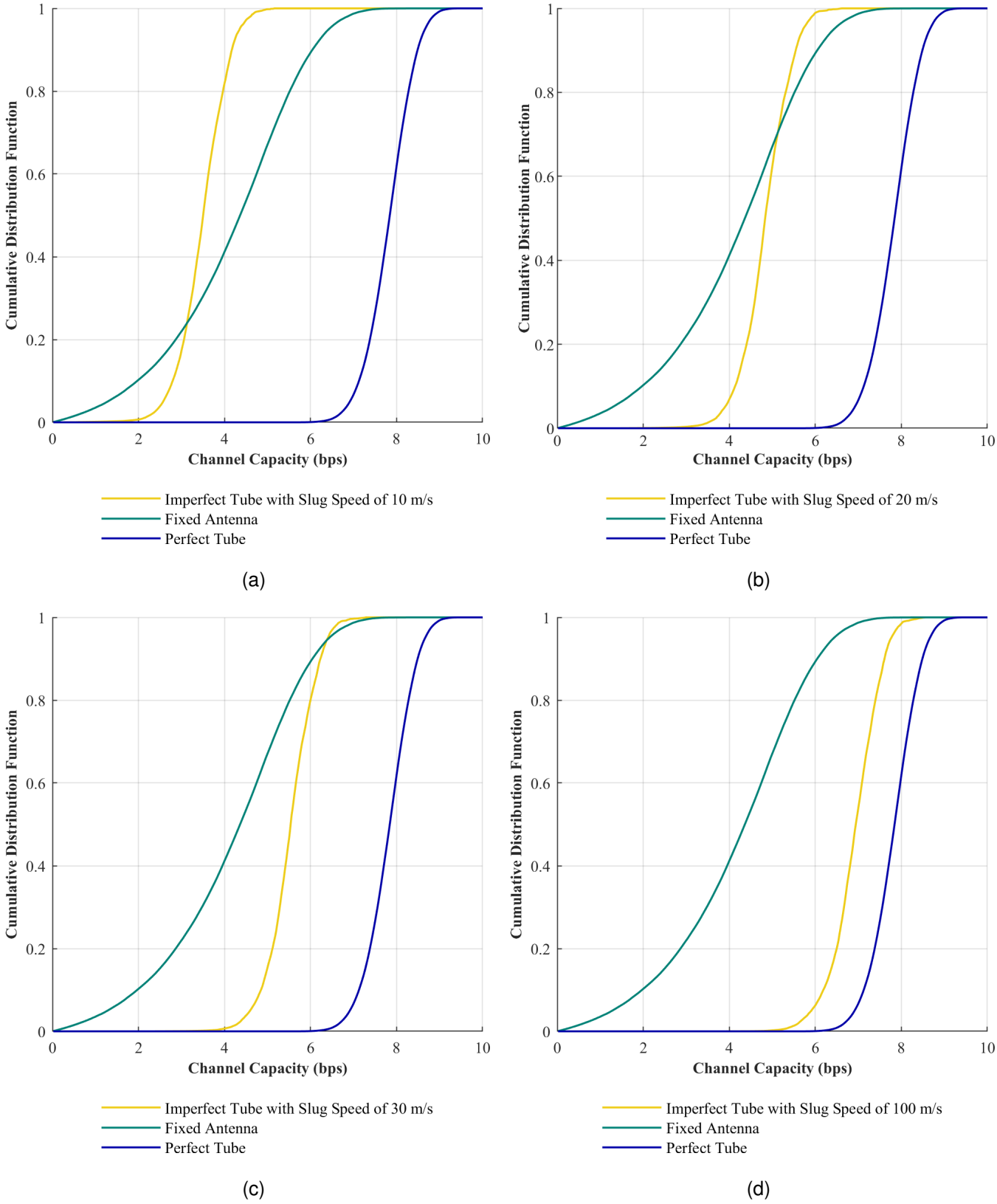

Fig. 3. Simulation results with the slug speed of the imperfect tube set to: (a) 10 ms^{-1}; (b) 20 ms^{-1}; (c) 30 ms^{-1}; and (d) 100 ms^{-1}.

REFERENCES

[1] S. Loyka, and J. Mosig, "Information theory and electromagnetism: Are they related?," in *MIMO System Technology for Wireless Communications*, Boca Raton, FL, USA, 2006, pp. 57–88.

[2] PC Magazine, "Exclusive: On LTE performance, iPhone 11 Pro Ties iPhone XS," [Online]. Available: https://www.pcmag.com/news/exclusive-on-lte-performance-iphone-11-pro-ties-iphone-xs

[3] K. K. Wong, A. Shojaeifard, K. F. Tong, and Y. Zhang, "Fluid antenna systems," *IEEE Transactions on Wireless Communications*, vol. 20, pp. 1950–1962, March 2021.

[4] K. K. Wong, K. F. Tong, Y. Zhang, and Z. Zhongbin, "Fluid antenna system for 6G: When Bruce Lee inspires wireless communications," *Electron. Lett.*, vol. 56, no. 24, pp. 1288-1290, 2020.

[5] V. C. Chen, H. Ling, and H. Ling, *Time-frequency transforms for radar imaging and signal analysis*. Norwood, USA, Artech House, 2002, pp. 12-13.

[6] K. K. Wong, K. F. Tong, Y. Shen, Y. Chen, and Y. Zhang, "Bruce Lee-inspired fluid antenna system: Six research topics and the potentials for 6G," *Front. Comms. Net.*, vol. 3, pp. 1–31, March 2022.

[7] H. Holma, and H. Viswanathan, "In the 6G era, we won't need to sacrifice sustainability for the sake of performance," [Online]. Available: https://www.bell-labs.com/institute/blog/in-the-6g-era-wewont-need-to-sacrifice-sustainability-for-the-sake-of-performance, November 2022.

[8] F. Gray, D.A. Kramer, and J.D. Bliss, "Gallium and gallium compounds," *Kirk-Othmer Encycl. Chem. Technol.*, vol. 12, pp. 337-364, DOI:10.1002/0471238961.0701121219010215.a01.pub2.

[9] K. K. Wong, and K. F. Tong, "Fluid antenna multiple access," in *IEEE Transactions on Wireless Communications*, vol. 21, no. 7, pp. 4801-4815, July 2022, DOI: 10.1109/TWC.2021.3133410.

[10] Z. Chai, K.-K. Wong, K.-F. Tong, Y. Chen and Y. Zhang, "Port selection for fluid antenna systems," in *IEEE Communications Letters*, vol. 26, no. 5, pp. 1180-1184, 2022.

[11] N. Waqar, K. K. Wong, K. F. Tong, A. Sharples, and Y. Zhang, "Deep learning enabled slow fluid antenna multiple access," in *IEEE Communications Letters*, vol. 27, no. 3, pp. 861-865, March 2023, DOI: 10.1109/LCOMM.2023.3237595.

[12] R. Wang, Y. Chen, Y. Hou, K. K. Wong and X. Tao, "Estimation of channel parameters for port selection in millimeter-wave fluid antenna systems," in *2023 IEEE/CIC International Conference on Communications in China (ICCC Workshops)*, Dalian, China, 2023, pp. 1-6, DOI: 10.1109/ICCCWorkshops57813.2023.10233765.

[13] C. Skouroumounis, and I. Krikidis, "Fluid antenna with linear MMSE channel estimation for large-scale cellular networks," in *IEEE Transactions on Wireless Communications*, vol. 71, pp. 1112–1125, February 2023.

[14] [12] J. B. Nielsen, R. L. Hanson, H. M. Almughamsi, C. Pang, T. R. Fish, and A. T. Woolley, "Microfluidics: Innovations in materials and their fabrication and functionalisation," *Anal. Chem.*, vol. 92, no. 1, pp. 150–168, Nov. 2019, DOI: 10.1021/acs.analchem.9b04986.

[15] [13] Y. W. Wu, S. Alkaraki, S. Y. Tang, Y. Wang, and J. R. Kelly, "Circuits and antennas incorporating gallium-based liquid metal," in *Proceedings of the IEEE*, vol. 111, no. 8, pp. 955-977, Aug. 2023, DOI: 10.1109/JPROC.2023.3285400.

[16] S. Y. Tang *et al.*, "Electrochemically induced actuation of liquid metal marbles," *Nanoscale*, vol. 5, no. 13, pp. 5949–5957, 2013, DOI: 10.1039/C3NR00185G.

[17] A. J. Evans, ENGR489 Engineering Project, (2023), GitLab repository, Available: https://gitlab.ecs.vuw.ac.nz/course-work/project489/2023/evansadri2/engr489

[18] S. R. Saunders, and A. Aragon-Zavala *Antennas and propagation for wireless communication systems*. West Sussex, U.K., John Wiley & Sons, 2007, p. 237.

[19] N. Costa, and S. Haykin *Multiple-input multiple-output channel models: Theory and practice*. New York, USA, Wiley Telecom, 2010, p. 99.

[20] W. C. Jakes, *Microwave Mobile Communications*. Piscataway, NJ, USA: IEEE Press, 1974, p. 329.

[21] J. P. Kermoal, L. Schumacher, K. I. Pedersen, P. E. Mogensen, and F. Frederiksen, "A stochastic MIMO radio channel model with experimental validation," in *IEEE Journal on Selected Areas in Communications*, vol. 20, no. 6, pp. 1211-1226, Aug. 2002, doi: 10.1109/JSAC.2002.801223.

[22] M. Hunukumbure, J. P. Coon, B. Allen, and T. Vernon, *The Technology and Business of Mobile Communications*. West Sussex, U.K., John Wiley & Sons, 2022, p. 155.